Thermal Management Enables Bright and Stable Perovskite Light Emitting Diodes

*Lianfeng Zhao[1], Kwangdong Roh[1], Sara Kacmoli[1], Khaled Al Kurdi,[2] Samik Jhulki[2], Stephen Barlow[2], Seth R. Marder[2], Claire Gmachl[1], and Barry P. Rand[1,3]**

Dr. L. Zhao, Dr. K. Roh, S. Kacmoli, Prof. C. Gmachl, Prof. B. P. Rand
Department of Electrical Engineering, Princeton University, Princeton, NJ 08544, USA

K. Al Kurdi, Dr. S. Jhulki, Dr. S. Barlow, Prof. S. R. Marder
School of Chemistry and Biochemistry, Center for Organic Electronics, Georgia Institute of Technology, Atlanta, GA 30332-0400, USA

Prof. B. P. Rand
Andlinger Center for Energy and the Environment, Princeton University, Princeton, NJ 08544, USA

E-mail: brand@princeton.edu

Keywords: organic-inorganic hybrid perovskites, perovskite light emitting devices, thermal management, efficiency roll-off, device stability

Abstract

The performance of lead-halide perovskite light-emitting diodes (LEDs) has increased rapidly in recent years. However, most reports feature devices operated at relatively small current densities (<500 mA/cm^2) with moderate radiance (<400 W/sr·m^2). Here, Joule heating and inefficient thermal dissipation are shown to be major obstacles towards high radiance and long lifetime. Several thermal management strategies are proposed in this work, such as doping charge-transport layers, optimizing device geometry, and attaching heat spreaders and sinks. Combining these strategies, high-performance perovskite LEDs are demonstrated with maximum radiance of 2555 W/sr·m^2, peak external quantum efficiency (EQE) of 17%, considerably reduced EQE roll-off (EQE > 10% to current densities as high as 2000 mA/cm^2), and tenfold increase in operational lifetime (when driven at 100 mA/cm^2). Furthermore, with proper thermal management, a maximum current density of 2.5 kA/cm^2 and an EQE of approximately 1% at 1

kA/cm^2 are shown using electrical pulses, which represents an important milestone towards electrically driven perovskite lasers.

Main text

For an LED technology to be practical, long lifetime, particularly at high radiance, is required for both display and lighting applications. In particular, the microLED technology,[1] which has attracted growing interest from the display industry in recent years, requires higher brightness that only devices made from inorganic III-V materials are capable of reaching to-date. Light emitting devices based on metal halide perovskites, on the other hand, hold potential in achieving high brightness due to their high charge-carrier mobility and less severe Auger loss (at least compared to organic materials).[2] Despite the rapid improvement in performance,[3] perovskite LEDs with brightness comparable to inorganic LEDs have yet to be reported. One source of this difficulty is that the external quantum efficiency (EQE) of perovskite LEDs typically decreases at high current densities (or brightness), an effect known as EQE roll-off. The origins of EQE roll-off remain controversial, but have been attributed to Auger recombination, electrical filed induced quenching, Joule heating, and charge imbalance.[2, 4] Furthermore, operational lifetime decreases dramatically at high current densities,[5] making it difficult to achieve both high brightness and long lifetime.

Efforts have been made to minimize EQE roll-off and improve lifetime,[4a, 6] mainly through modifications to the perovskite composition. We have shown recently that the performance of perovskite LEDs is sensitive to temperature, and that elevated temperature caused by Joule heating is a major factor contributing to device degradation.[5] In this work, we show that Joule heating also plays a substantial role in the EQE roll-off. Several thermal management strategies are applied to perovskite LEDs, resulting in record high radiance, greatly

reduced EQE roll-off, and significantly improved operational lifetime. Furthermore, metal halide perovskites hold great potential as gain media for realizing non-epitaxial electrically driven laser diodes.[7] Several milestones towards this goal have been achieved, such as the realization of optically pumped lasing from complete and functional LED structures with embedded distributed feedback resonators,[8] and the demonstration of optically pumped continuous-wave (CW) amplified spontaneous emission (ASE) and lasing.[9] However, EQE roll-off and device degradation significantly hold back the achievement of high current densities required for electrically driven lasing. In this work, we show the importance of thermal management towards the realization of electrically pumped lasing, and demonstrate pulsed operation of perovskite LEDs at a record high current density of 2.5 kA/cm^2 and much improved EQEs in the kiloampere per square centimeter range.

The perovskite LED structure used in this work comprises indium tin oxide (ITO)/polyTPD (15 nm)/$MAPbI_3$ perovskite (40 nm)/$POPy_2$ (40 nm)/Ag, where polyTPD is poly(4-butyltriphenylamine-4',4"-diyl), MA is methylammonium, and $POPy_2$ is phenyldi(pyren-2-yl)phosphine oxide. The perovskite layer was prepared using an established in-situ perovskite nanocrystalline film preparation technique.[3c,10] The addition of 20 mol% bulky benzylammonium iodide additives allows us to prepare smooth (about 1 nm surface roughness), pin-hole free perovskite thin films without altering the 3D $MAPbI_3$ tetragonal crystal structure.[11] The thickness of the perovskite layer (40 nm) was optimized for efficient light-outcoupling.[5] **Figure 1**a shows the detailed structure, where polyTPD is used as a hole-transport layer (HTL), and $POPy_2$ is used as an electron-transport layer (ETL). The thickness of each layer is confirmed by the cross-sectional transmission electron microscopy image shown in Figure 1b and energy-dispersive X-ray spectroscopy (EDX) elemental mapping in Supplementary Figure S1. Four

thermal management strategies were used to reduce Joule heating and facilitate heat dissipation. Firstly, we used doped ETLs and HTLs to increase device conductivity and thus reduce Joule heating. Specifically, $POPy_2$ was n-doped with the molecular reductant (pentamethylcyclopentadienyl)(1,3,5-trimethylbenzene)ruthenium dimer ($[RuCp^*Mes]_2$)[12] and polyTPD was p-doped with the electron-acceptor molecule 2,3,5,6-tetrafluoro-7,7,8,8-tetracyanoquinodimethane (F_4-TCNQ).[13] Figure 1c shows the molecular structures of polyTPD, $POPy_2$, F_4-TCNQ and $[RuCp^*Mes]_2$. The p-doping mechanism of F_4-TCNQ for poly-TPD follows traditional charge-transfer doping mechanisms for organic molecules (Supplementary Figure S2). The n-doping mechanism of $[RuCp^*Mes]_2$ for $POPy_2$ are detailed in our previous work.[12] After doping, the conductivity is increased from ~10^{-8} S/m to ~10^{-2} S/m for the $POPy_2$ layer and from ~0.01 S/m to ~0.04 S/m for the polyTPD layer.[12-13] Secondly, we attached additional heat spreaders and heat sinks on top of the Ag electrodes and used more thermally conductive sapphire wafers as substrates instead of glass. Specifically, we used a graphite sheet (50 μm thick, thermal conductivity of 1300 W/m·K) with an insulating acrylic adhesive layer (6 μm thick) (Supplementary Figure S3) or a polycrystalline diamond (300 μm thick, thermal conductivity >2000 W/m·K) as the heat spreader, and a copper bar as a heat sink. Thirdly, we defined a narrow line-shape device geometry to reduce total power consumption and increase heat dissipation. Finally, we drove the device with electrical pulses instead of a continuous electrical bias. We show how these strategies improve device performance, especially at high current densities.

We first compare the performance of perovskite LEDs with doped or undoped ETLs and HTLs, as shown in **Figure 2**. The electroluminescence (EL) spectra and angular-dependent emission intensity profiles are shown in Supplementary Figure S4. After doping, a marked

increase in current density and radiance is observed at a given voltage after device turn-on (Figure 2a and b), and the EQE roll-off is much reduced (Figure 2c). Similar peak EQEs of 17.0% and 16.4% are achieved for the undoped and doped devices, respectively. This indicates that the electron-hole balance is not altered significantly for the optimized doping conditions of the ETLs and HTLs; however, we noticed reduced EQEs when using a higher doping concentration in the HTLs. The device lifetime increases dramatically after doping, possibly due to reduced Joule heating. As shown in Figure 2d, T_{50} (the time taken for the EQE or light intensity to drop to half of its initial value) driven at a constant current density of 10 mA/cm^2 is increased from 10 to 117 min, which represents a tenfold improvement. In fact, the significant effects of electronic and thermal conductivity of charge transport layers on device lifetime could explain the long lifetime of previously reported perovskite LEDs with ZnO ETLs.[3e, 14] Note that besides the reduced Joule heating, which we believe is the major contributor to the improved stability in this work, there might be other possible mechanisms responsible for this improvement, such as fluorine-induced hydrogen bond formation with the ammonium hydrogen in $MAPbI_3$ perovskites at the HTL/perovskite interface,[11] which deserves further investigation and clarification.

To further improve thermal dissipation, based on the doped ETL and HTL device structure we replaced the glass substrate with sapphire and attached a graphite heat spreader and a copper heat sink on top of the Ag electrode (structure shown in Figure 1a). **Figure 3**a and b show the radiance and EQE curves for devices with different areas and thermal management strategies. The current density–voltage (*J–V*) curves are shown in Supplementary Figure S5. Performance is very similar for devices with or without applying these thermal management strategies when driven below 500 mA/cm^2. The EQE droop in this region sources from changes

to the electron-hole balance. However, when operated at current densities above 500 mA/cm^2, Joule heating is the dominant factor for the rapid EQE roll-off for devices without thermal management, whereas devices with improved thermal management are able to operate beyond 5000 mA/cm^2 with significantly reduced EQE roll-off (with an EQE of 10% being maintained at 2000 mA/cm^2). Notably, with these strategies, we achieve a maximum radiance of 1323 W/sr·m^2 at a current density of 3.7 A/cm^2. To our knowledge, this is the first report of perovskite LEDs reliably operating in the ampere per square centimeter range, which shows the potential of perovskites in high-power applications such as lighting or microLEDs, or ultimately electrically pumped lasers.

A performance comparison between a 10 and 2.5 mm^2 area perovskite LED in Figure 3a and b confirms that device area plays a significant role in heat dissipation. To further demonstrate the potential of perovskite LEDs at high current densities, we patterned the device area using an insulating SiO_2 layer (Supplementary Figure S6). In particular, we prepared a device with a 4 μm × 1 mm line-shape current aperture geometry, a sapphire substrate, a graphite heat spreader, and a copper heat sink. Such a device reaches a maximum radiance of 2555 W/sr·m^2 and a maximum current density of 25 A/cm^2 (Figure 3c and d). This size-dependent performance improvement indicates that micron-sized perovskite LEDs might be promising in practical display and lighting applications. The graphite heat spreader performs better than the diamond possibly because the soft adhesive layer forms a better thermal contact to the LED than the rigid diamond. Note that EQE roll-off is worsened in the relatively small current density regions (e.g., below 2500 mA/cm^2) for these SiO_2 patterned devices compared to devices without the SiO_2 layer. This is possibly because the SiO_2 patterning layer changed the thickness and uniformity of the spin-coated polyTPD and/or perovskite layers, thereby slightly altering charge

balance. We are not exclusively attributing the EQE roll-off to Joule heating, but showing that Joule heating plays a significant role in the EQE roll-off, especially when roll-off occurs at high current densities.

We also investigated the operational lifetime of perovskite LEDs with thermal management strategies (**Figure 4**). When driven at a constant current density of 100 mA/cm^2 (corresponding to an initial radiance of 75 W/sr·m^2), a tenfold improvement in operational lifetime (T_{50} from 0.52 h to 5.45 h) is achieved after attaching a graphite heat spreader and copper heat sink (Figure 4a). The thermal management strategies play a more significant role at higher current densities, conditions where more heat is generated. A hundred-fold improvement in operational lifetime (T_{50} from 4 to 436 s) is observed when driven at 800 mA/cm^2 (corresponding to an initial radiance of 450 W/sr·m^2) (Figure 4b). Figure 4c shows the stabilized carrier temperatures during device operation extracted from the high-energy EL tails (Supplementary Figure S7) according to the generalized Planck equation.[9a, 15] Heat builds up significantly for devices without applying thermal management strategies. For example, carrier temperature increases dramatically to approximately 110 °C for a 10 mm^2 LED driven at 200 mA/cm^2. In contrast, carrier temperature maintains a moderate level of approximately 50 °C for a 2.5 mm^2 LED with the graphite heat spreader, even driven at a high current density of 1000 mA/cm^2. To further reduce the influence of heat buildup on device lifetime, we tested device stability using electrical pulses with a pulsing width (PW) of 2 μs and a duty cycle of 20% (Supplementary Figure S8). This allows the device to cool between each pulse. Figure 4d shows the time evolution of the normalized EQE under pulsed operation at 800 mA/cm^2. No EQE degradation is observed during the first 7500 s, corresponding to 1500 s in effective time (total pulse “on” time), which is significantly longer than that under continuous current drive.

We further studied the effects of thermal management for perovskite LEDs operated at extremely high current densities driven by electrical pulses (Supplementary Figure S9). **Figure 5**a shows normalized radiance–time curves for perovskite LEDs driven by a 700 A/cm^2 pulse with a pulsing width of 800 ns. The EL intensity decreased to approximately 70% of its initial value within the 800 ns pulse duration for a device fabricated on a glass substrate due to significant Joule heating[16] even within such a short pulse, consistent with previously reported results.[2] In contrast, only 10% decrease in EL intensity is observed for a device fabricated on a sapphire substrate, and no EL intensity change is observed over the pulse for a device with the graphite heat spreader. Note that the high frequency noise in the radiance measurements of the pulsed devices is purely due to incomplete electromagnetic shielding of the detection circuit. It has been left unfiltered in order to illustrate the fast response time of the device. Figure 5b and c show the radiance–current density curves and EQE–current density curves of perovskite LEDs driven in the pulsed mode. Significantly higher radiances and EQEs are achieved after applying the thermal management strategies, especially at high current densities exceeding 1 kA/cm^2. Notably, we achieved an EQE of approximately 1% at 1 kA/cm^2 and a maximum radiance of 59026 W/sr·m^2 at 2 kA/cm^2. Based on an estimated threshold carrier density $n_{\mathrm{th}} \approx 8\mathrm{x}10^{17}$cm^{-3} for a $MAPbI_3$ perovskite laser in a distributed feedback resonator,[15a] the threshold current density can be estimated as $J_{\mathrm{th}} \approx q d_0 B n_{\mathrm{th}}^2 / \eta_{\mathrm{IQE}}$,[2] where q is the elementary charge, $d_0 \approx 40$ nm is the thickness of the perovskite layer, $B \approx 4\mathrm{x}10^{-10}$ cm^{3}s^{-1} is the bimolecular radiative rate constant for $MAPbI_3$,[17] and η_{IQE} is the internal quantum efficiency of the perovskite LED. Based on a typical outcoupling efficiency $\phi_{\mathrm{oc}} = \eta_{\mathrm{EQE}} / \eta_{\mathrm{IQE}} \approx 0.2$, the corresponding EQE-current density product at the lasing threshold would be $\eta_{\mathrm{EQE}} J_{\mathrm{th}} \approx 33$ A/cm^2. In comparison, we reached a peak $\eta_{\mathrm{EQE}} J \approx 10$ A/cm^2, demonstrating that the injection level needed for lasing is

realistically feasible. It should be noted, however, the elevated carrier temperature (Supplementary Figure S10) will further increase the lasing threshold.[8] Although no sign of stimulated emission is observed yet (Supplementary Figure S11), our work represents an important milestone towards electrically driven perovskite lasers.

In summary, we have shown the importance of thermal management in perovskite LEDs, and proposed several effective thermal management strategies. Based on these, we are able to show perovskite LEDs with record high radiance, much reduced EQE roll-off and significantly improved operational lifetime. Furthermore, these thermal management strategies have allowed us to operate perovskite LEDs at extremely high current densities driven by electrical pulses, an important step towards electrically driven perovskite lasers.

Experimental Section

Materials: Methylammonium iodide (MAI) and benzylammonium iodide (PMAI) were purchased from Greatcell Solar. PbI_2 was purchased from Alfa Aesar. PolyTPD was purchased from American Dye Source. $POPy_2$ was purchased from Lumtec. F_4-TCNQ was purchased from Ossila. $[RuCp^*Mes]_2$ was synthesized as described elsewhere.[18] Dimethylformamide, chlorobenzene, and toluene were purchased from Sigma-Aldrich. The graphite sheet with an insulating adhesive layer was manufactured by Panasonic. All materials were used as received.

Device fabrication: The perovskite precursor solution was prepared in a N_2 filled glovebox by dissolving MAI, PbI_2 and PMAI in DMF to obtain 0.2 M $MAPbI_3$ with 0.04 M PMAI as an additive. The precursor solution was used within three hours of fully dissolving. Perovskite LEDs were fabricated using ITO (Lumtec) coated glass or sapphire substrates with a sheet resistance of 15 Ω/sq. Substrates were cleaned in air sequentially with soapy water, deionized water, acetone, and isopropyl alcohol, and were then treated with O_2 plasma for 10 min prior to film deposition in a N_2 filled glovebox. PolyTPD (4.8 mg/ml in chlorobenzene), with or without

the F_4-TCNQ dopant (0.2 mg/ml in chlorobenzene), was spin coated on top of ITO at 1500 rpm for 70 s, followed by thermal annealing at 150 °C for 20 min. Samples were then treated with O_2 plasma for 15 s to improve wettability for the perovskite layer spin-coated on top at 6000 rpm. A solvent-quenching step was performed after 4 s by dropping toluene (100 μL) on the spinning samples.[10] The samples were annealed at 70 °C for 5 min. Then, 10 nm undoped $POPy_2$, 30 nm $POPy_2$ doped with $[RuCp^*Mes]_2$ (in a ratio of 6:1) and 100 nm Ag electrodes were thermally evaporated on top of the perovskite films to complete device fabrication. For the undoped ETL control devices, after the deposition of 30 nm undoped $POPy_2$, another 10 nm doped $POPy_2$ were deposited to keep the same ETL thickness and carrier-injection barrier from the Ag electrodes. All devices were illuminated at one-sun intensity (AM 1.5G, 100 mW/cm^2) using a solar simulator for 10 min to photoactivate the n-dopant.[12] The device area is defined either by the overlap between ITO and Ag electrodes, or by a patterned insulating SiO_2 (120 nm) layer. To pattern SiO_2 on ITO, photoresist (AZ1518) was spin-coated at 4000 rpm for 40 s on an ITO/glass or ITO/sapphire substrate. After baking the photoresist layer at 95 °C for 60 s, positive photolithography was carried out, followed by development for 60 s. An insulating 120 nm-thick SiO_2 layer was grown by plasma enhanced chemical vapor deposition at 70 °C. The small-area LED pattern was finally obtained by lift-off and then soaking the sample in photoresist remover (AZ1165) at 80 °C overnight.

Characterization: Perovskite LEDs were measured in a N_2 glovebox using a custom motorized goniometer consisting of a Keithley 2400 sourcemeter unit, a picoammeter (4140B, Agilent), a calibrated Si photodiode (FDS-100-CAL, Thorlabs), and a calibrated fiber optic spectrophotometer (UVN-SR, StellarNet Inc.). For the pulsed measurement, LEDs were encapsulated with encapsulation epoxy (Lumtec) in conjunction with glass coverslips in a N_2-

filled glovebox before transferring out. A voltage pulse train was generated from a pulse pattern generator and applied to the LEDs. Current was determined by measuring the voltage across a 50 Ohm termination resistor using an oscilloscope. EL intensity was measured using a Si amplified photodetector and an oscilloscope. The EQE was determined from the EL intensity and current density near the end of each pulse. Cross-section TEM lamellar samples of the LEDs were prepared by an FEI Helios DualBeam microscope. Cross-sectional TEM images and EDX measurements were carried out in an FEI Talos (S)TEM at 200 kV. Morphologies of the graphite sheet and the patterned SiO_2 layer were surveyed by an FEI Verios 460 XHR SEM.

Supporting Information
Supporting Information is available from the Wiley Online Library or from the author.

Acknowledgements
We thank Prof. Stephen Y. Chou at Princeton University for suggesting the graphite heat sink. This work is supported by the Air Force Office of Scientific Research under Award No. FA9550-18-1-0037 and the National Science Foundation under DMR-1807797. S. J. thanks the United States-India Educational Foundation (USIEF, India) and Institute of International Education (IIE, USA) for a Fulbright-Nehru Postdoctoral Fellowship (Grant No. 2266/FNPDR/2017). The authors acknowledge the use of Princeton's Imaging and Analysis Center, which is partially supported by the Princeton Center for Complex Materials, a National Science Foundation (NSF)-MRSEC program (DMR-1420541).

Received: ((will be filled in by the editorial staff))
Revised: ((will be filled in by the editorial staff))
Published online: ((will be filled in by the editorial staff))

References

[1] H. Jiang, J. Lin, *Opt. Express* **2013**, *21*, A475.
[2] H. Kim, L. Zhao, J. S. Price, A. J. Grede, K. Roh, A. N. Brigeman, M. Lopez, B. P. Rand, N. C. Giebink, *Nat. Commun.* **2018**, *9*, 4893.
[3] a) Z.-K. Tan, R. S. Moghaddam, M. L. Lai, P. Docampo, R. Higler, F. Deschler, M. Price, A. Sadhanala, L. M. Pazos, D. Credgington, *Nat. Nanotechnol.* **2014**, *9*, 687; b) H. Cho, S.-H. Jeong, M.-H. Park, Y.-H. Kim, C. Wolf, C.-L. Lee, J. H. Heo, A. Sadhanala, N. Myoung, S. Yoo, *Science* **2015**, *350*, 1222; c) Z. Xiao, R. A. Kerner, L. Zhao, N. L. Tran, K. M. Lee, T.-W. Koh, G. D. Scholes, B. P. Rand, *Nat. Photonics* **2017**, *11*, 108; d) M. Yuan, L. N. Quan, R. Comin, G. Walters, R. Sabatini, O. Voznyy, S. Hoogland, Y.

Zhao, E. M. Beauregard, P. Kanjanaboos, *Nat. Nanotechnol.* **2016**, *11*, 872; e) Y. Cao, N. Wang, H. Tian, J. Guo, Y. Wei, H. Chen, Y. Miao, W. Zou, K. Pan, Y. He, *Nature* **2018**, *562*, 249; f) B. Zhao, S. Bai, V. Kim, R. Lamboll, R. Shivanna, F. Auras, J. M. Richter, L. Yang, L. Dai, M. Alsari, *Nat. Photonics* **2018**, *12*, 783; g) T. Chiba, Y. Hayashi, H. Ebe, K. Hoshi, J. Sato, S. Sato, Y.-J. Pu, S. Ohisa, J. Kido, *Nat. Photonics* **2018**, *12*, 681; h) X. Zhao, Z.-K. Tan, *Nat. Photonics* **2019**, *14*, 215.

[4] a) W. Zou, R. Li, S. Zhang, Y. Liu, N. Wang, Y. Cao, Y. Miao, M. Xu, Q. Guo, D. Di, *Nat. Commun.* **2018**, *9*, 608; b) F. Yuan, Z. Wu, H. Dong, B. Xia, J. Xi, S. Ning, L. Ma, X. Hou, *Appl. Phys. Lett.* **2015**, *107*, 261106.

[5] L. Zhao, K. M. Lee, K. Roh, S. U. Z. Khan, B. P. Rand, *Adv. Mater.* **2019**, *31*, 1805836.

[6] Y. Shang, Y. Liao, Q. Wei, Z. Wang, B. Xiang, Y. Ke, W. Liu, Z. Ning, *Sci. Adv.* **2019**, *5*, eaaw8072.

[7] W. B. Gunnarsson, B. P. Rand, *APL Mater.* **2020**, *8*, 030902.

[8] H. Kim, K. Roh, J. P. Murphy, L. Zhao, W. B. Gunnarsson, E. Longhi, S. Barlow, S. R. Marder, B. P. Rand, N. C. Giebink, *Adv. Opt. Mater.* **2020**, *8*, 1901297.

[9] a) Y. Jia, R. A. Kerner, A. J. Grede, B. P. Rand, N. C. Giebink, *Nat. Photonics* **2017**, *11*, 784; b) P. Brenner, O. Bar-On, M. Jakoby, I. Allegro, B. S. Richards, U. W. Paetzold, I. A. Howard, J. Scheuer, U. Lemmer, *Nat. Commun.* **2019**, *10*, 1.

[10] R. A. Kerner, L. Zhao, Z. Xiao, B. P. Rand, *J. Mater. Chem. A* **2016**, *4*, 8308.

[11] a) L. Zhao, N. Rolston, K. M. Lee, X. Zhao, M. A. Reyes-Martinez, N. L. Tran, Y.-W. Yeh, N. Yao, G. D. Scholes, Y.-L. Loo, A. Selloni, R. H. Dauskardt, B. P. Rand, *Adv. Funct. Mater.* **2018**, *28*, 1802060; b) L. Zhao, Y.-W. Yeh, N. L. Tran, F. Wu, Z. Xiao, R. A. Kerner, Y. L. Lin, G. D. Scholes, N. Yao, B. P. Rand, *ACS Nano* **2017**, *11*, 3957.

[12] X. Lin, B. Wegner, K. M. Lee, M. A. Fusella, F. Zhang, K. Moudgil, B. P. Rand, S. Barlow, S. R. Marder, N. Koch, A. Kahn, *Nat. Mater.* **2017**, *16*, 1209.

[13] M.-H. Tremblay, K. Schutt, Y. Zhang, J. Lim, Y.-H. Lin, J. H. Warby, S. Barlow, H. J. Snaith, S. R. Marder, *Sustain. Energy Fuels* **2020**, *4*, 190.

[14] W. Xu, Q. Hu, S. Bai, C. Bao, Y. Miao, Z. Yuan, T. Borzda, A. J. Barker, E. Tyukalova, Z. Hu, *Nat. Photonics* **2019**, *13*, 418.

[15] a) Y. Jia, R. A. Kerner, A. J. Grede, A. N. Brigeman, B. P. Rand, N. C. Giebink, *Nano Lett.* **2016**, *16*, 4624; b) J. Shah, R. C. C. Leite, *Phys. Rev. Lett* **1969**, *22*, 1304; c) P. Wurfel, *J. Phys. C: Solid State Phys.* **1982**, *15*, 3967.

[16] Z. Shi, S. Li, Y. Li, H. Ji, X. Li, D. Wu, T. Xu, Y. Chen, Y. Tian, Y. Zhang, *ACS Nano* **2018**, *12*, 1462.

[17] R. L. Milot, G. E. Eperon, H. J. Snaith, M. B. Johnston, L. M. Herz, *Adv. Funct. Mater.* **2015**, *25*, 6218.

[18] H. I. Un, S. A. Gregory, S. K. Mohapatra, M. Xiong, E. Longhi, Y. Lu, S. Rigin, S. Jhulki, C. Y. Yang, T. V. Timofeeva, *Adv. Energy Mater.* **2019**, *9*, 1900817.

Figures

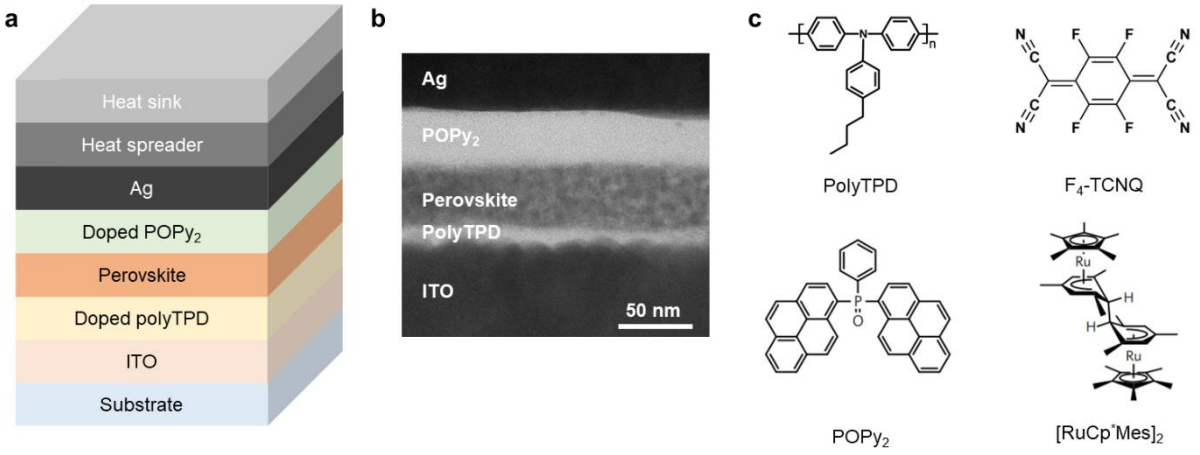

Figure 1. Device structure and thermal management designs for perovskite light-emitting diodes. a, Schematic diagram of a perovskite LED employing thermal management strategies. **b**, Cross-sectional TEM image of a perovskite LED. **c**, Molecular structures of polyTPD, $POPy_2$, F_4-TCNQ and $[RuCp^*Mes]_2$, used for the HTL, ETL, p-dopant and n-dopant, respectively.

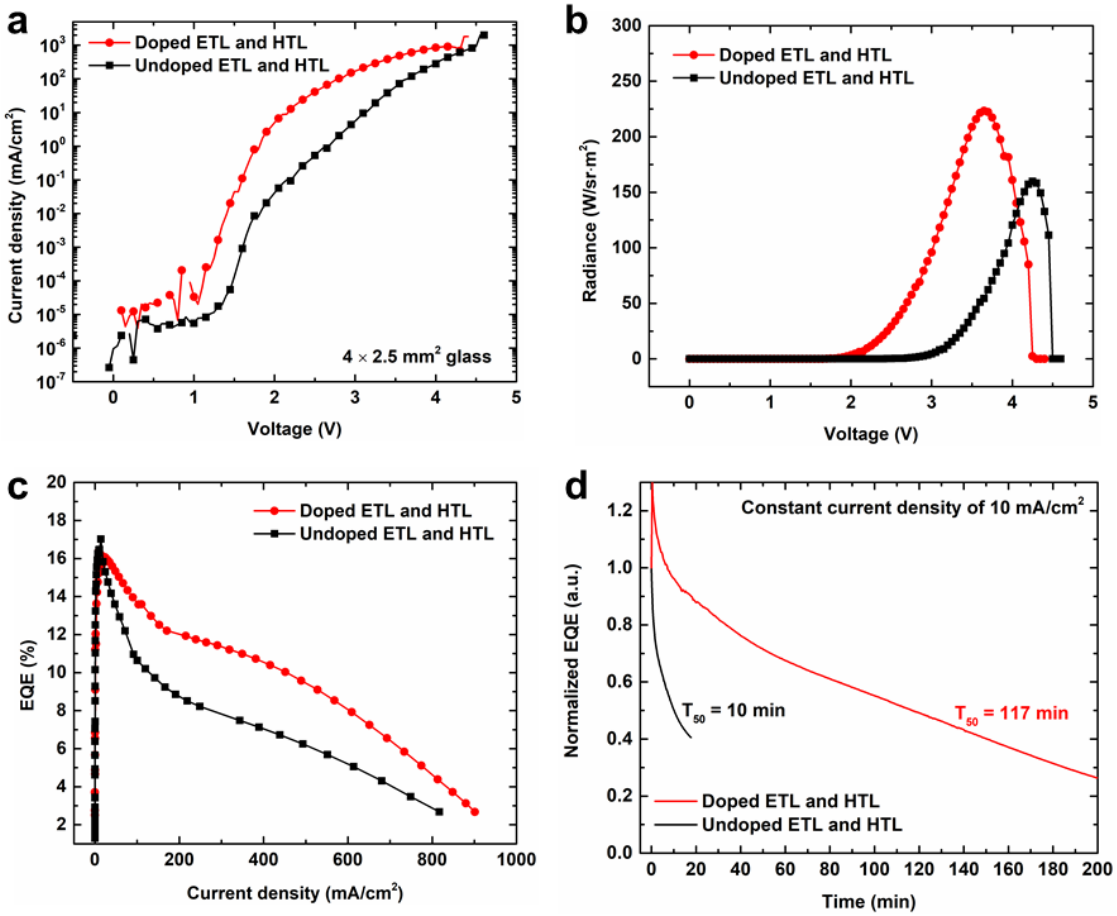

Figure 2. Characteristics of perovskite LEDs with doped or undoped ETL and HTL. a-c, Current density–voltage curves (**a**), radiance–voltage curves (**b**), and EQE–current density curves (**c**) of perovskite LEDs with doped or undoped ETL and HTL. **d**, Lifetime test of perovskite LEDs at a constant current density of 10 mA/cm^2.

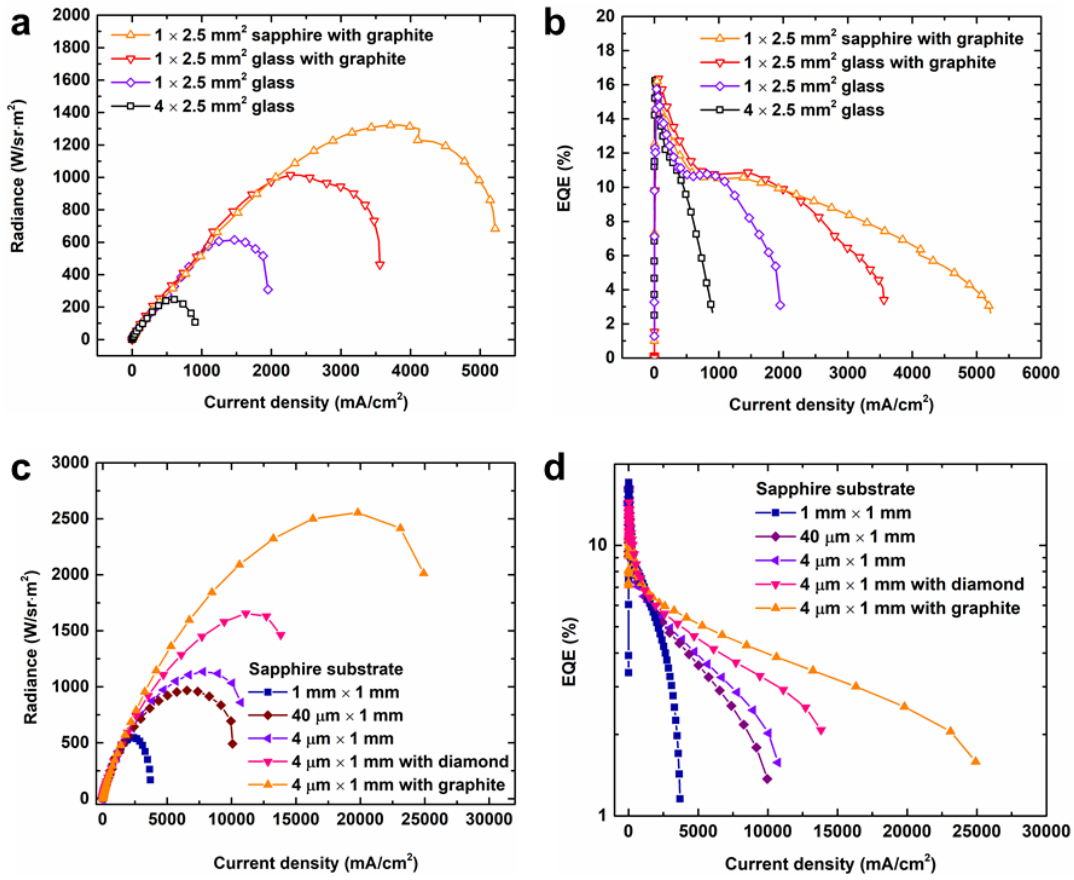

Figure 3. Characteristics of perovskite LEDs with various geometry, substrate and heat spreaders. a,b, radiance–current density curves (**a**) and EQE–current density curves (**b**) of perovskite LEDs on glass or sapphire substrates, with or without a graphite heat spreader and copper heat sink. The 2.5 or 10 mm^2 active area is defined by the overlap between the ITO and Ag electrodes. **c,d,** radiance–current density curves (**c**) and EQE–current density curves (**d**) of perovskite LEDs on sapphire substrates, with or without a graphite or diamond heat spreader and copper heat sink. The active areas in (c) and (d) are defined by insulating and patterned SiO_2.

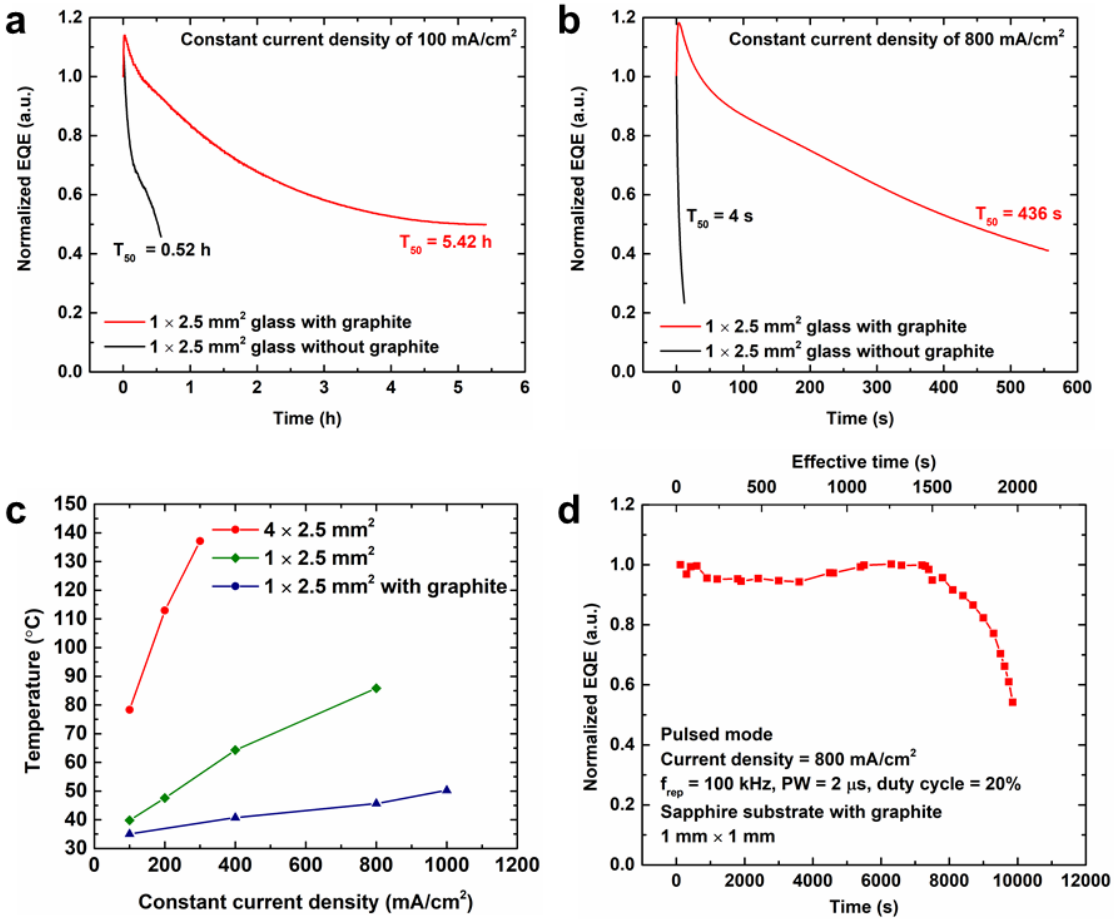

Figure 4. Operational lifetime. a,b, Time evolution of the normalized EQE of perovskite LEDs at a constant current density of (**a**) 100 mA/cm^2 and (**b**) 800 mA/cm^2. **c**, Carrier temperature extracted from the high-energy electroluminescence tail for perovskite LEDs with various geometry and heat spreaders as a function of constant current density. **d**, Time evolution of the normalized EQE of a perovskite LED under pulsed operation at 800 mA/cm^2. The pulse repetition rate is 100 kHz with 20% duty cycle.

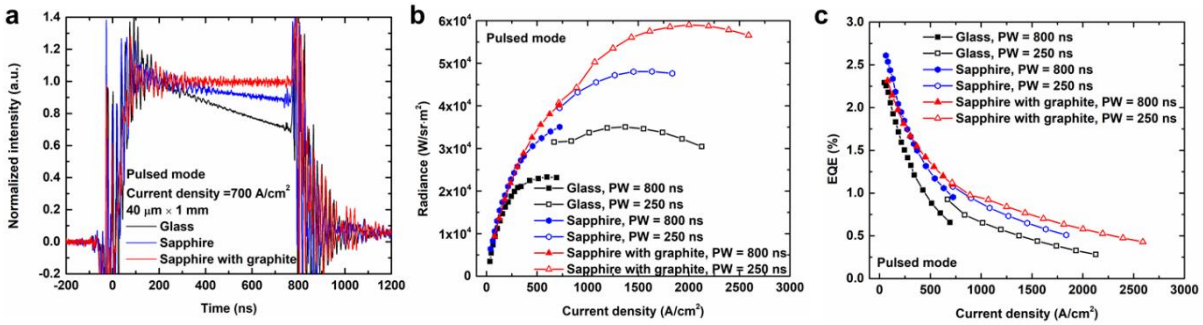

Figure 5. Pulsed operation of perovskite LEDs at high current densities. a, Normalized radiance–time curves for perovskite LEDs driven by a 700 A/cm^2 pulse with a pulsing width of 800 ns. **b**,**c**, Radiance–current density curves (**b**) and EQE–current density curves (**c**) of perovskite LEDs on glass or sapphire substrates, with or without a graphite heat spreader and copper heat sink, all driven in pulsed mode.

The table of contents entry

Several thermal management strategies are proposed and applied to perovskite light emitting diodes (LEDs), resulting in greatly reduced efficiency roll-off, record high radiance, and significantly improved operational lifetime. Furthermore, these thermal management strategies have enabled pulsed operation of perovskite LEDs in the kiloampere per square centimeter range with much improved device performance, an important step towards electrically driven perovskite lasers.

Keywords: **organic-inorganic hybrid perovskites, perovskite light emitting devices, thermal management, efficiency roll-off, device stability**

L. Zhao, K. Roh, S. Kacmoli, K. Al Kurdi, S. Jhulki, S. Barlow, S. R. Marder, C. Gmachl, B. P. Rand*

Thermal Management Enables Bright and Stable Perovskite Light Emitting Diodes

ToC figure